Table VI. UV-Visible Absorbance of $[((p\text{-X})TPP)Ag^{III}]^+$ in Me_2SO, 0.1 M TBAP

porphyrin	λ, nm (ε × 10^{-4}, cm^{-1} M^{-1})		
$[((p\text{-CN})TPP)Ag^{III}]^{+a}$	427 (14.9)	536 (2.0)	
$[((p\text{-Cl})TPP)Ag^{III}]^{+a}$	426 (10.9)	537 (1.8)	
$[(TPP)Ag^{III}]^{+b}$	428 (17)	537 (1.6)	
$[((p\text{-}OC_2H_5)TPP)Ag^{III}]^{+b}$	452 (14)	546 (3.1)	578 (2.0)
$[((p\text{-}OCH_3)TPP)Ag^{III}]^{+a}$	449 (8.8)	543 (2.0)	580 (sh)

[a] Chemically generated with $Ce(SO_4)_2$. [b] Electrochemically generated.

to significantly influence the Ag(II)/Ag(III) reaction.

Table VI shows spectral data for five different $((p\text{-X})TPP)Ag^{III}$ complexes that were chemically or electrochemically generated by oxidation of $((p\text{-X})TPP)Ag^{II}$ in Me_2SO. As seen in this table, the electron-donating groups have the strongest substituent effect on the Ag(III) spectra. Only small shifts of the absorption peaks occur for $[((p\text{-X})TPP)Ag]^+$ where X = CN, Cl, or H. However, a shift of about 20 nm occurs for the Ag(III) complexes that contain porphyrins with X = OCH_3 or OC_2H_5. No explanation for this shift is available at present, but this may be related to the effect of Me_2SO coordination.

In summary, this study has presented the first detailed electrochemical and spectral characterizations of silver porphyrin electrode reactions in nonaqueous media. Eleven different complexes of $((p\text{-X})TPP)Ag$ were investigated in three different solvent systems. It is significant to note that the electrochemically generated Ag(I) porphyrins were sufficiently stable in Me_2SO and py so that they could be spectrally characterized. These complexes could also be further reduced to form the anion radicals without demetalation.

Acknowledgment. The support of the National Science Foundation (Grant No. CHE-8515411) is gratefully acknowledged.

Registry No. $((p\text{-}NO_2)TPP)Ag$, 102682-18-8; $((p\text{-}NO_2)TPP)Ag^+$, 102682-24-6; $((p\text{-}NO_2)TPP)Ag^{2+}$, 102682-29-1; $((p\text{-}NO_2)TPP)Ag^-$, 102682-37-1; $((p\text{-CN})TPP)Ag$, 102682-19-9; $((p\text{-CN})TPP)Ag^+$, 102696-36-6; $((p\text{-CN})TPP)Ag^{2+}$, 102682-30-4; $((p\text{-CN})TPP)Ag^-$, 102682-38-2; $((p\text{-CN})TPP)Ag^{2-}$, 102682-47-3; $((p\text{-}CF_3)TPP)Ag$, 102682-20-2; $((p\text{-}CF_3)TPP)Ag^+$, 102682-25-7; $((p\text{-}CF_3)TPP)Ag^{2+}$, 102682-31-5; $((p\text{-}CF_3)TPP)Ag^-$, 102682-39-3; $((p\text{-Cl})TPP)Ag$, 75964-88-4; $((p\text{-Cl})TPP)Ag^+$, 77761-16-1; $((p\text{-Cl})TPP)Ag^{2+}$, 102682-32-6; $((p\text{-Cl})TPP)Ag^-$, 102682-40-6; $((p\text{-F})TPP)Ag$, 76500-30-6; $((p\text{-F})TPP)Ag^+$, 77701-69-0; $((p\text{-F})TPP)Ag^{2+}$, 102696-37-7; $((p\text{-F})TPP)Ag^-$, 102682-41-7; $(TPP)Ag$, 14641-64-6; $(TPP)Ag^+$, 101567-28-6; $(TPP)Ag^{2+}$, 77701-68-9; $(TPP)Ag^-$, 59980-02-8; $((p\text{-}CH_3)TPP)Ag$, 75964-91-9; $((p\text{-}CH_3)TPP)Ag^+$, 77761-15-0; $((p\text{-}CH_3)TPP)Ag^{2+}$, 102682-33-7; $((p\text{-}CH_3)TPP)Ag^-$, 102682-42-8; $((p\text{-}OC_2H_5)TPP)Ag$, 102682-21-3; $((p\text{-}OC_2H_5)TPP)Ag^+$, 102682-26-8; $((p\text{-}OC_2H_5)TPP)Ag^{2+}$, 102682-34-8; $((p\text{-}OC_2H_5)TPP)Ag^-$, 102682-43-9; $((p\text{-}OCH_3)TPP)Ag$, 75964-92-0; $((p\text{-}OCH_3)TPP)Ag^+$, 77701-66-7; $((p\text{-}OCH_3)TPP)Ag^{2+}$, 102682-35-9; $((p\text{-}OCH_3)TPP)Ag^-$, 102682-44-0; $((p\text{-}OCH_2C_6H_5)TPP)Ag$, 102682-22-4; $((p\text{-}OCH_2C_6H_5)TPP)Ag^+$, 102682-27-9; $((p\text{-}OCH_2C_6H_5)TPP)Ag^{2+}$, 102682-36-0; $((p\text{-}OCH_2C_6H_5)TPP)Ag^-$, 102682-45-1; $((p\text{-}NEt_2)TPP)Ag$, 102682-23-5; $((p\text{-}NEt_2)TPP)Ag^+$, 102682-28-0; $((p\text{-}NEt_2)TPP)Ag^-$, 102682-46-2; Ce, 7440-45-1; hydrazine, 302-01-2.

Contribution from the Department of Chemistry,
The University of Houston—University Park, Houston, Texas 77004

Electrochemistry, Spectroelectrochemistry, and Ligand Addition Reactions of an Easily Reducible Cobalt Porphyrin. Reactions of (Tetracyanotetraphenylporphinato)cobalt(II) ($((CN)_4TPP)Co^{II}$) in Pyridine and in Pyridine/Methylene Chloride Mixtures

X. Q. Lin, B. Boisselier-Cocolios, and K. M. Kadish*

Received April 3, 1986

The electrochemistry, spectroelectrochemistry, and pyridine binding reactions of $((CN)_4TPP)Co^{II}$ were investigated in nine nonaqueous solvents. The four electron-withdrawing CN groups on the porphyrin ring lead to extremely facile reductions such that three one-electron additions could be observed within the range of the solvent. The first reduction occurred between −0.21 and −0.51 V vs. SCE and was assigned as due to formation of Co(II) anion radical. This is in contrast to reduction of unsubstituted $(TPP)Co^{II}$ where the formation of Co(I) is postulated to occur. The second reduction of $((CN)_4TPP)Co$ occurs between −0.80 and −0.94 V vs. SCE and is assigned as due to formation of a Co(I) anion radical. Finally, the third reduction occurs between −1.72 and −1.78 V vs. SCE and is assigned as due to formation of a Co(I) dianion. All three reductions were monitored by thin-layer spectroelectrochemistry, and the spectrum of each reduction product was obtained. A spectrum of electrooxidized $((CN)_4TPP)Co^{II}$ was also obtained in pyridine and methylene chloride. The former solvent is the only one in which a well-defined Co(II) ⇄ Co(III) transition was observed. In addition, the electrochemistry and pyridine binding reactions of $((CN)_4TPP)Co$ were investigated in CH_2Cl_2/pyridine mixtures. Values of $E_{1/2}$ for each electrode reaction were monitored as a function of pyridine concentration, and on the basis of these data, an overall oxidation-reduction and ligand addition scheme was formulated. Stability constants were measured for the stepwise addition of two pyridine molecules to $((CN)_4TPP)Co^{II}$ and $[((CN)_4TPP)Co^{III}]^+$. Similar magnitudes of formation constants were obtained by using electrochemical and spectral methods to monitor the ligand binding reactions of Co(II). Both mono- and bis(pyridine) adducts to Co(II) were identified by electronic absorption spectroscopy.

Introduction

Electrochemical studies of cobalt porphyrins have been the subject of numerous publications.[1-3] Nearly 20 years ago, Stanienda and Biebl[4] first reported potentials for oxidation of several synthetic cobalt(II) porphyrins in nonaqueous media. Three one-electron oxidations were observed. These reactions were later assigned as due to the Co(II)/Co(III) couple followed by the reversible formation of a Co(III) cation radical and a Co(III) dication at more positive potentials.[5-8]

Reductions of Co(II) porphyrins in nonaqueous media have also been studied in great detail.[5,6,9-12] The first electroreduction

(1) Kadish, K. M. *Prog. Inorg. Chem.* **1986**, *34*, 435-605.
(2) Felton, R. H. In *The Porhyrins*; Dolphin, D., Ed.; Academic: New York, 1978; Vol. V, Chapter 3.
(3) Davis, D. G. In *The Porphyrins*; Dolphin, D., Ed.; Academic: New York, 1978; Vol. V, Chapter 4.
(4) Stanienda, A.; Biebl, G. *Z. Phys. Chem. (Munich)* **1967**, *52*, 254.
(5) Walker, F. A.; Beroiz, D.; Kadish, K. M. *J. Am. Chem. Soc.* **1976**, *98*, 3484.
(6) Truxillo, L. A.; Davis, D. G. *Anal. Chem.* **1975**, *47*, 2260.
(7) Wolberg, A. *Isr. J. Chem.* **1974**, *12*, 1031.
(8) Wolberg, A.; Manassen, J. *J. Am. Chem. Soc.* **1970**, *92*, 2982.
(9) Felton, R. H.; Linschitz, M. *J. Am. Chem. Soc.* **1966**, *88*, 1113.
(10) Kadish, K. M.; Davis, D. G. *Ann. N.Y. Acad. Sci.* **1973**, *206*, 495.

0020-1669/86/1325-3242$01.50/0 © 1986 American Chemical Society

corresponds to the Co(II)/Co(I) electrode reaction. A second reduction has been reported to occur between −1.87 and −1.92 V vs. SCE for (TPP)Co (where TPP is the dianion of tetraphenylporphyrin), but this reaction has not been investigated in any detail. This is due in large part to the extreme reactivity of the doubly reduced species, which is formed very close to the solvent window of most nonaqueous electrochemical solvents.

Reported half-wave potentials for the oxidation of different cobalt(II) porphyrins range between 0.782 and −0.21 V vs. SCE.[4-15] Values of $E_{1/2}$ or E_p have been related to the basicity (pK_a) of the bound axial ligand[14,15] as well as to the coordinating ability of the aprotic solvent.[5,6] Oxidation potentials of Co(II) porphyrins are also dependent upon the type and the concentration of supporting electrolyte.[5-7,14] The shift of $E_{1/2}$ for Co(II) $\rightleftarrows$ Co(III) has been attributed to differences in the strength of the Co(III)–axial ligand interaction for complexes with different axially bound ligands or different axially bound solvent molecules.[12] Co(III) preferentially forms six-coordinate complexes with nitrogenous bases while Co(II) almost invariably binds only a single nitrogenous base. A bis-ligated Co(II) complex has been postulated on the basis of spectroscopic data[16-20] and a bis(pyridine) adduct has been suggested to be the electroactive species in neat pyridine.[21]

In this present paper we have characterized the ligand addition reactions and electrochemistry of (tetracyanotetraphenylporphinato)cobalt(II) (((CN)$_4$TPP)Co). Unlike phenyl-substituted cobalt tetraphenylporphyrins, ((*p*-X)TPP)Co,[5] the four CN groups in ((CN)$_4$TPP)Co are linked directly to the porphyrin macrocycle and this results in large changes in electrochemical reactivity. The electrochemistry of several different tetracyano-substituted tetraphenylporphyrins has been reported in the literature.[22-26] In all cases the four electron-withdrawing CN groups result in large changes of porphyrin ring basicity such that extremely facile reductions are possible. Positive shifts in $E_{1/2}$ by up to 1.0 V are observed upon going from (TPP)M to ((CN)$_4$TPP)M, thus resulting in easily generated anion radicals and dianions of the tetracyano-substituted complex.

Additional reductions may also occur for the tetracyano-substituted complexes that are not observed for the unsubstituted or para-substituted tetraphenylporphyrins. For example, ((CN)$_4$TPP)Cu[25] and ((CN)$_4$TPP)FeCl[26] both undergo three single-electron additions, one of which corresponds to the generation of a stable Cu(I) or Fe(I) complex. ((CN)$_4$TPP)Co can also undergo three reductions, one of which will correspond to the generation of a Co(I) species. As expected the compound is characterized as having extremely easy reductions due to the highly electron withdrawing CN groups. Two reductions and no oxidations have been reported at a dropping Hg electrode,[22] but up to three reductions and one oxidation are observed at a Pt electrode. This present study examines these electrode reactions in CH_2Cl_2, pyridine, CH_2Cl_2/pyridine mixtures, and in seven other nonaqueous solvents. Formation constants for the addition of pyridine to ((CN)$_4$TPP)Co and [((CN)$_4$TPP)Co^{III}]$^+$ in CH_2Cl_2 were determined. Formation of a cobalt(II) porphyrin anion radical has not previously been suggested in the literature and is spectrally characterized for the first time in this study.

Thin-layer spectroelectrochemistry was also carried out in order to provide spectral characterization of each electrooxidized and electroreduced species. A self-consistent electrode mechanism is proposed, and comparisons are made between the reactions of (TPP)Co and ((CN)$_4$TPP)Co under the same solution conditions.

Experimental Section

Instrumentation. Cyclic voltammograms were obtained with an IBM Model EC 225 voltammetric analyzer and an Omigraphic 2000 X-Y recorder. A three-electrode system was used. The working electrode was a platinum-button electrode with a surface area of about 0.8 mm^2. A commercial saturated calomel electrode (SCE) was used as the reference electrode. This aqueous reference electrode was separated from the bulk solution by an asbestos-tipped glass frit, which also functioned as a Luggin capillary for more accurate potential measurements with minimal *IR* loss. An expanded platinum electrode with about 1 cm^2 surface area was used as the auxiliary electrode. A homemade vacuum-tight electrochemical cell with solution volume of about 5 mL was used for monitoring cyclic voltammograms during titrations with pyridine. High-purity N_2 was passed through a degasser that contained the relevant solvent. N_2 was bubbled through the bulk solution to remove any oxygen and was blown over the solution surface to maintain an N_2 atmosphere during experiments. Electronic *IR* compensation built into the instrumentation was used in order to obtain more accurate potential measurements.

Spectroelectrochemical experiments were carried out by using a vacuum-tight short path length thin-layer spectroelectrochemical cell with a doublet platinum-gauze working electrode. The design of this cell is described in the literature.[13] A Tracor Northern TN-1710 multichannel analyzer was combined with a TN-1710-24 floppy disk system for spectral acquisitions. In order to reduce noise, 100 acquisitions were automatically averaged over a 0.5-s period.

Electronic absorption spectra of the neutral complexes were also obtained with an IBM 9430 UV–visible spectrophotometer. A 1 cm path length quartz cell with a specially designed plastic cap was used for the phototitration cell. For the purpose of deoxygenation, dry N_2 gas was introduced into the sample chamber of this instrument.

Chemicals. (TPP)Co^{II} was either synthesized and characterized according to well-known procedures[5] or was obtained from Strem Chemical Co. No difference was found between the different sources of the compounds. Free-base ((CN)$_4$TPP)H$_2$ was synthesized according to the method of Callot,[24] and insertion of cobalt into the porphyrin core was accomplished by using the method described by Giraudeau et al.[22] Methylene chloride (CH_2Cl_2) (analytical grade, Fisher Scientific Co.) was freshly distilled from P_2O_5 before use. Pyridine (py) (Fisher Scientific Co.) and dimethyl sulfoxide (Me_2SO) (Aldrich Chemical Co.) were freshly distilled from CaH_2 under argon. *N*,*N*-Dimethylformamide (DMF), propylene carbonate (PC), and *N*-methylformamide (NMF) (Aldrich Chemical Co.) were freshly distilled from activated 4-Å molecular sieves under vacuum. Tetrahydrofuran (THF) (Fisher Scientific Co.) was first distilled from CaH_2, and then further purified by a following distillation over sodium–benzophenone. *N*,*N*-Dimethylacetamide (DMA) and hexamethylphosphoramide (HMP) (Aldrich Chemical Co.) were distilled over BaO under vacuum. Tetrabutylammonium perchlorate (TBAP) (Fluka Chemical Co.) was used as the supporting electrolyte and was recrystallized from ethanol and dried in vacuo prior to use.

Methods. Changes in axial coordination upon electron transfer were determined by shifts in the half-wave potential as a function of the ligand concentration. The spectroelectrochemical and electrochemical methods for calculating formation constants have been described in a previous paper.[12] Both the bulk solution and the frit solution were titrated simultaneously. Also, in order to avoid dilution effects, both the titrant and titrated solution were prepared with the same concentration of supporting electrolyte and sample compound. Under these experimental conditions there was no change in liquid-junction potential between CH_2Cl_2 and CH_2Cl_2 containing less than 0.5 M pyridine. This was ascertained by measuring $E_{1/2}$ of the ferrocene/ferrocenium couple in solutions of different CH_2Cl_2/pyidine ratios.

Results and Discussion

Spectral Characterization of ((CN)$_4$TPP)Co(py) and ((CN)$_4$TPP)Co(py)$_2$. Formation constants for mono- and bis(pyridine) addition to Co(II) and Co(III) porphyrins have been

(11) Lexa, D.; Lhoste, J. M. *Experientia, Suppl.* **1971**, *8*, 395.
(12) Kadish, K. M; Bottomley, L. A.; Beroiz, D. *Inorg. Chem.* **1978**, *17*, 1124.
(13) Lin, X. Q.; Kadish, K. M. *Anal. Chem.* **1985**, *57*, 1498.
(14) Gaudemer, J. A.; Boucly-Goester, C.; Boucly, P. *Inorg. Chem.* **1982**, *21*, 3413.
(15) Carter, M. J.; Englehardt, L. M.; Rillema, D. P.; Basolo, F. *J. Chem. Soc., Chem. Commun.* **1973**, 810.
(16) Walker, F. A. *J. Am. Chem. Soc.* **1970**, *92*, 4235.
(17) Walker, F. A. *J. Am. Chem. Soc.* **1973**, *95*, 1150.
(18) Wayland, B. B.; Abd-Elmageed, M. E. *J. Am. Chem. Soc.* **1974**, *96*, 4809.
(19) Stynes, H. C.; Ibers, J. A. *J. Am. Chem. Soc.* **1972**, *94*, 1559.
(20) Dokuzovic, Z.; Ahmeti, X.; Pavlovic, D.; Murati, I.; Asperger, S. *Inorg. Chem.* **1982**, *21*, 1576.
(21) Carter, M. J.; Rillema, D. P.; Basolo, F. *J. Am. Chem. Soc.* **1974**, *96*, 392.
(22) Giraudeau, A.; Callot, H. J.; Jordan, J.; Ezhar, I.; Gross, M. *J. Am. Chem. Soc.* **1979**, *101*, 3857.
(23) Giraudeau, A.; Callot, H. J.; Gross, M. *Inorg. Chem.* **1979**, *18*, 201.
(24) Callot, H. J.; Giraudeau, A.; Gross, M. *J. Chem. Soc., Perkin Trans. 1* **1975**, *2*, 1321.
(25) Giraudeau, A.; Louati, A.; Gross, M.; Callot, H. J.; Hanson, L. K.; Rhodes, R. K.; Kadish, K. M. *Inorg. Chem.* **1982**, *21*, 1581.
(26) Kadish, K. M.; Boisselier-Cocolios, B.; Simonet, B.; Chang, D.; Ledon, H.; Cocolios, P. *Inorg. Chem.* **1985**, *24*, 2148.

Table I. Spectral Data for the Various $((CN)_4TPP)Co^{II}$ Complexes

overall complex charge	proposed complex	solvent	λ_{max}, nm ($\epsilon \times 10^{-3}$, cm^{-1} M^{-1})				
0	$((CN)_4TPP)Co^{II}$	CH_2Cl_2	434 (143)	626 (37)			
	$((CN)_4TPP)Co^{II}(py)$	8×10^{-3} M py/CH_2Cl_2	426 (121)	470 (39)	627 (19)		
	$((CN)_4TPP)Co^{II}(py)_2$	1.0 M py/CH_2Cl_2	440 (120)	446 (125)	627 (24)		
		py	438 (120)	448 (125)	629 (25)		
+1	$[((CN)_4TPP)Co^{III}]^+$	CH_2Cl_2	463 (92)		652 (29)		
	$[((CN)_4TPP)Co^{III}(py)_2]^+$	py	472 (132)		672 (22)		
−1	$[((CN)_4TPP)Co^{II}]^-$	CH_2Cl_2	440 (77)	485 (sh)	589 (33)	663 (sh)	710 (sh)
	$[((CN)_4TPP)Co^{II}(py)]^-$	py	438 (61)	449 (62)	489 (42)	601 (11)	
−2	$[((CN)_4TPP)Co^{I}]^{2-}$	py	443 (53)	585 (28)	629 (29)	690 (sh)	
		CH_2Cl_2	440 (41)	483 (sh)	589 (24)	663 (16)	
−3	$[((CN)_4TPP)Co^{I}]^{3-}$	py	450 (23)	580 (16)	629 (22)	683 (23)	

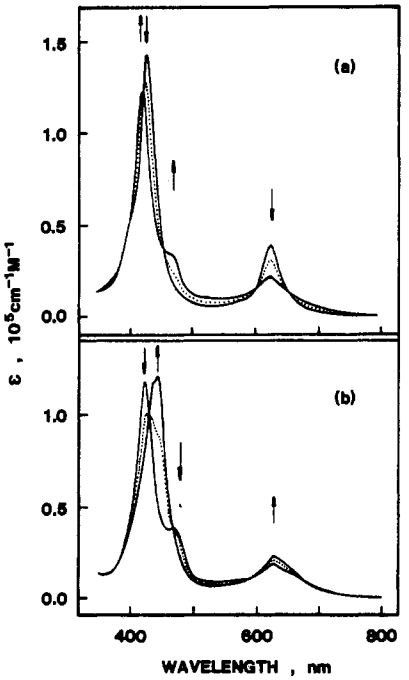

Figure 1. Spectral changes associated with the stepwise addition of pyridine to 4.5×10^{-6} M $((CN)_4TPP)Co$ in CH_2Cl_2: (a) first ligand addition occurring from [py] = 0 to 8×10^{-3} M; (b) second ligand addition occurring from [py] = 8×10^{-3} to 12.4 M.

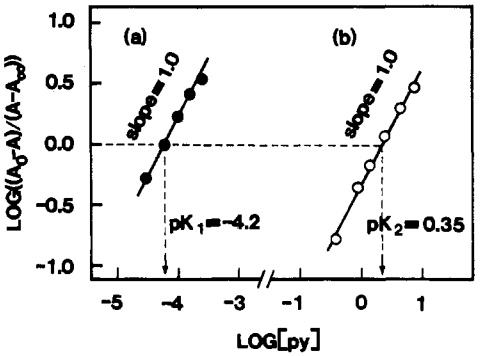

Figure 2. Logarithmic analysis of the spectral data in Figure 1 for the addition of pyridine to (a) $((CN)_4TPP)Co^{II}$ and $((CN)_4TPP)Co^{II}(py)$ in CH_2Cl_2. The first ligand addition step (●) was monitored at 630 nm while the second step (○) was monitored at 446 nm.

Table II. Formation Constants for Pyridine Binding in CH_2Cl_2

complex	log K_1	log K_2	log β_2
$((CN)_4TPP)Co^{II}$	4.2[a]	−0.35[a]	3.8[a]
	4.9[b]	−0.36[b]	4.5[b]
$(TPP)Co^{II}$	2.88[c]		
	2.90[d]	[e]	
$[((CN)_4TPP)Co^{III}]^+$	8.3[b]	9.2[b]	17.5[b]
$[(TPP)Co^{III}]^+$			15.6[c]

[a] From spectral data. [b] From electrochemical data. [c] Reference 28. Value spectrally determined in toluene. [d] Reference 12. Value electrochemically determined in CH_2Cl_2. [e] No reaction.

measured in several solvents.[12,27-30] In this present study, the stepwise binding of one and two pyridine ligands to $((CN)_4TPP)Co^{II}$ was demonstrated by spectrophotometrically monitoring addition of pyridine to the complex in CH_2Cl_2. These results are shown in Figure 1.

The initial $((CN)_4TPP)Co$ complex a Soret band at 434 nm and a single band in the visible region located at 626 nm. However, as the concentration of pyridine in CH_2Cl_2 is increased to 8 mM, the Soret band shifts to 426 nm and a new peak appears at 470 nm. At the same time the Q-band at 626 nm decreases in intensity and shifts slightly to 627 nm. This is shown in Figure 1a.

The second step in the titration of $((CN)_4TPP)Co$ is also well-defined and is characterized by the disappearance of the first set of isosbestic points at 404, 430, 460, 606, and 656 nm and the appearance of the second set of isosbestic points at 370, 432, 468, 596, and 676 nm. As the pyridine concentration is increased above 8.0×10^{-3} M, the Soret band at 426 nm decreases in intensity while a split peak appears at 440 and 446 nm. At the same time the Q-band increases slightly. This is shown in Figure 1b. All of these data indicate a two-step reaction with pyridine as shown in eq 1 and 2, where P = $(CN)_4TPP$. Spectra data for the neutral

$$(P)Co^{II} + py \rightleftarrows (P)Co^{II}(py) \quad (1)$$

$$(P)Co^{II}(py) + py \rightleftarrows (P)Co^{II}(py)_2 \quad (2)$$

$((CN)_4TPP)Co^{II}$ complex and for the mono- and bis(pyridine) adducts in CH_2Cl_2 are summarized in Table I. Logarithmic analyses of the spectrophotometric data are shown in Figure 2 and give formation overall constants of $10^{4.2}$ and $10^{3.8}$ for the mono- and bis(pyridine) adducts, respectively. These values are listed in Table II.

Electrochemistry of $((CN)_4TPP)Co$ in CH_2Cl_2 and in CH_2Cl_2/Pyridine Mixtures. Cyclic voltammograms of $((CN)_4TPP)Co$ were taken in CH_2Cl_2 solutions containing various concentrations of pyridine. Representative voltammograms in CH_2Cl_2, in pyridine/CH_2Cl_2 mixtures, and in neat pyridine are shown in Figure 3. $((CN)_4TPP)Co^{II}$ undergoes three well-defined redox processes, which occur at 0.88, −0.21, and −0.94 V vs. SCE in CH_2Cl_2. These processes are labeled as peaks 1–3 in Figure 3a. Process 1 has $E_{pa} - E_{pc}$ = 120 mV (at a scan rate of 100 mV/s) and indicates a quasi-reversible electron-transfer process. This process is assigned as oxidation of $((CN)_4TPP)Co^{II}$ to generate $[((CN)_4TPP)Co^{III}]^+$. Peaks 2 and 3 correspond to the stepwise reduction of $((CN)_4TPP)Co^{II}$ and are electrochemically reversible in that the peak separations approach the theoretical

(27) Stynes, D. V.; Stynes, H.; James, B. R.; Ibers, J. A. *J. Am. Chem. Soc.* **1973**, *95*, 1796.
(28) Walker, F. A. *J. Am. Chem. Soc.* **1973**, *95*, 1150.
(29) Walker, F. A. *J. Am. Chem. Soc.* **1973**, *95*, 1154.
(30) Rillema, D. P.; Wicker, C. M., Jr.; Morgan, R. D.; Barringer, L. F.; Scism, L. A. *J. Am. Chem. Soc.* **1982**, *104*, 1276.
(31) Scholtz, W. F.; Reed, C. A.; Lee, Y. J.; Scheidt, W. R.; Lang, G. *J. Am. Chem. Soc.* **1982**, *104*, 6791.

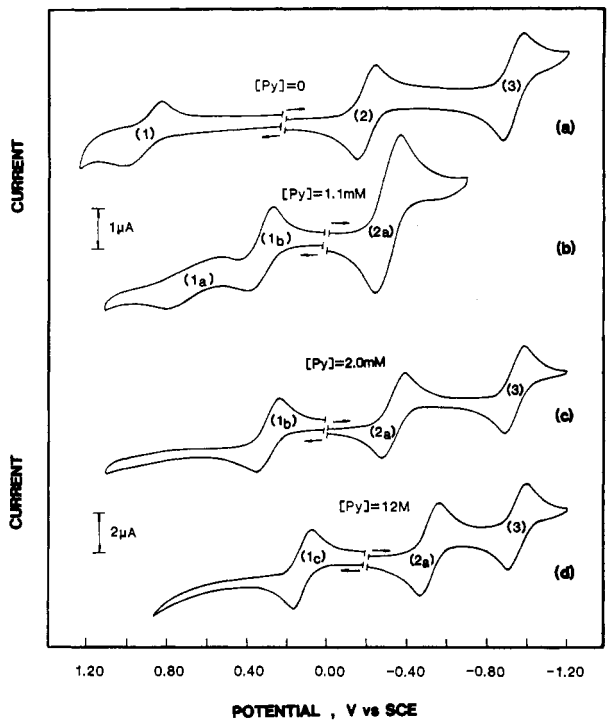

Figure 3. Cyclic voltammograms of 1.4×10^{-3} M $((CN)_4TPP)Co$ in (a) CH_2Cl_2, (b) 1.1×10^{-3} M py in CH_2Cl_2; (c) 2.0 mM py in CH_2Cl_2, and (d) neat pyridine. All solutions contain 0.1 M TBAP. Scan rate = 0.10 V/s.

peak to peak separation of 60 mV for a diffusion-controlled one-electron transfer.

The first oxidation of $((CN)_4TPP)Co^{II}$ in CH_2Cl_2 does not have a Nernstian reversible 60-mV separation of $|E_{pa} - E_{pc}|$ as shown in Figure 3a. In addition, the maximum peak currents are less than might be expected from a diffusion-controlled one-electron oxidation of $((CN)_4TPP)Co$ (see currents for reduction), thus suggesting the possibility of a rate-controlling chemical reaction preceding oxidation of Co(II). However, thin-layer spectral changes were recorded during a potential scan from 0.3 to 1.1 V and showed the reversible, quantitative conversion of $((CN)_4TPP)Co^{II}$ to $[((CN)_4TPP)Co^{III}]^+$. The electrogenerated Co(III) species has a well-defined Soret band at 463 nm and a Q-band at 652 nm. These values are listed in Table I.

A second oxidation step (not shown in Figure 3) also occurred at 1.30 V in CH_2Cl_2. This process was well-defined in a thin-layer cyclic voltammogram but was not spectrally monitored. This reaction is assigned as formation of the Co(III) cation radical, $[((CN)_4TPP)Co^{III}]^{2+}$, and can be compared with a similar reaction that occurs at $E_{1/2} = 0.97$ V for $[(TPP)Co^{III}]^{2+}$ formation in CH_2Cl_2.[13]

The currents for process 1 decreased as pyridine was added to CH_2Cl_2 and finally disappeared as the py concentration approached 1.1×10^{-3} M (~0.9 equiv of pyridine). At the same time two new oxidation peaks appeared at higher pyridine concentration. The first peak to appear was located at $E_{1/2} = 0.60$ V and did not shift with increasing pyridine concentration. This peak is also associated with a Co(II) $\rightleftarrows$ Co(III) reaction and is labeled as peak 1a in Figure 3b. The second oxidation peak (peak 1b) had an $E_{1/2}$ value that varied between 0.30 and 0.12 V, depending on the concentration of pyridine. This peak shifted by −59 mV per each 10-fold increase in pyridine concentration up to about 2.0 M pyridine. At this point, the peak stopped shifting. In neat pyridine the peak was found at $E_{1/2} = 0.12$ V vs. SCE and is labeled peak 1c.

Either one or two pyridine molecules may bind Co(III) and these reactions are given by eq 3 and 4, where P = $(CN)_4TPP$.

$$[(P)Co^{III}]^+ + py \rightleftarrows [(P)Co^{III}(py)]^+ \quad (3)$$

$$[(P)Co^{III}(py)]^+ + py \rightleftarrows [(P)Co^{III}(py)_2]^+ \quad (4)$$

Scheme I

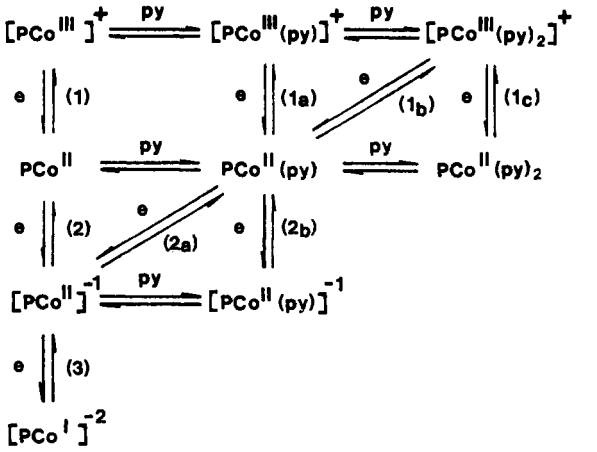

Two pyridine molecules can also be added to Co(II) (see preceding section), and these reactions are given by eq 1 and 2. Thus, a consideration of these types of complexation leads to the postulated reaction sequence shown in Scheme I. The oxidations in Scheme I are labeled as processes 1, 1a, 1b, or 1c while the reductions of $((CN)_4TPP)Co^{II}$ are labeled as processes 2, 2a, or 3. This notation is consistent with the voltammetric peaks shown in Figure 3.

Processes 1b, 2a, and 3 are well-defined and occur under a broad range of pyridine/CH_2Cl_2 mixtures. In contrast, peaks 1 and 2 occur only in neat CH_2Cl_2 while peak 1c occurs only in neat pyridine. These latter three peaks (1, 2, and 1c) are assigned on the basis of spectral data. On the other hand, less evidence exists for the assignment of peak 1a. This peak occurs at substoichiometric ratios of pyridine to porphyrin and is consistent with spectral data that indicates a mono(pyridine) Co(II) complex. However, the assignment of a final bis(pyridine) Co(III) product after reaction 1a is complicated by the fact that a dynamic equilibrium exists in solution and by the fact that there is not sufficient pyridine in solution to account for bis coordination by all of the Co(III) product. On the other hand, peak 1a does not shift with increase in pyridine concentration, and this can only be consistent with a lack of ligand exchange upon oxidation.

Verification of the other reaction pathways in Scheme I was accomplished by monitoring the shift of $E_{1/2}$ for each reaction as a function of an increase in pyridine concentration. Half-wave potentials of each reaction were measured as an average of the corresponding oxidation and reduction peak potentials, and plots of these half-wave potentials as a function of the py concentration are shown in Figure 4. From this figure, several linear segments with slopes of 0 or −59 mV can be identified. The titration curves with zero slope indicate no ligand exchange during the electron-transfer process. The titration curves with a −59-mV slope indicate a process where one ligand exchange has occurred during the oxidation. The assignment of a given reaction in Figure 4 is also consistent with the descriptions of the reactions given in Scheme I.

Formation constants for reactions 1–4 were determined by using electrochemical data of the type shown in Figure 4, and the calculated formation constants are listed in Table II. Also listed are formation constants for the addition of pyridine to $(TPP)Co^{II}$ and $[(TPP)Co^{III}]^+$ in CH_2Cl_2. The formation constants calculated for pyridine addition to $((CN)_4TPP)Co^{II}$ by electrochemical methods agree well with values determined by the spectrophotometric methods. The values of log K_1 are larger for $((CN)_4TPP)Co^{II}$ than for $(TPP)Co^{II}$ by over 1 order of magnitude. In addition, $((CN)_4TPP)Co^{II}$ shows clear evidence for binding of a second pyridine molecule in CH_2Cl_2. This is not the case for $(TPP)Co^{II}$, although bis(pyridine) adducts most likely exist in neat pyridine.

The overall log β_2 for binding of two pyridine molecules to $[((CN)_4TPP)Co^{III}]^+$ is larger than that for $[(TPP)Co^{III}]^+$ by 2 orders of magnitude. More importantly, however, a stepwise

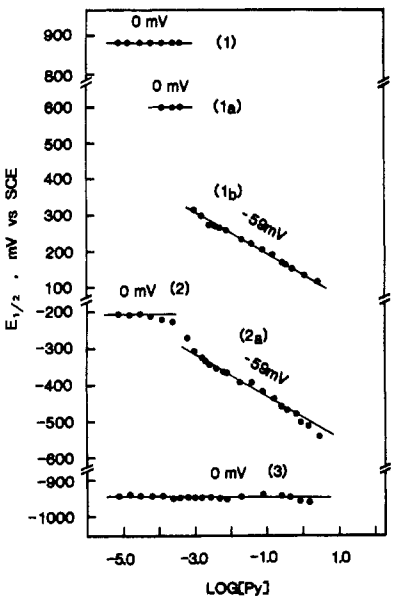

Figure 4. Dependence of $E_{1/2}$ on pyridine concentration for the oxidation and reduction of $((CN)_4TPP)Co$ in CH_2Cl_2/py mixtures. Processes 1–3 are identified in Figure 3 and in Scheme I.

binding by the former complex is electrochemically observed. This is not the case for pyridine binding to $(TPP)Co^{III}$, where only an overall log β_2 = 15.6 has been measured.

Spectral Identification of Oxidation–Reduction Products in Pyridine and in CH_2Cl_2. The reversible one-electron oxidation of $((CN)_4TPP)Co$ in pyridine occurs at 0.12 V (peak 1c, Figure 3d) while the reversible reductions occur at −0.51 (peak 2a) and −0.94 V (peak 3) vs. SCE. An additional reduction step also appears at −1.75 V. This reduction has not been reported in the literature and can be assigned as the second ring reduction of $[((CN)_4TPP)Co^{I}]^-$. It does not occur in CH_2Cl_2 but is seen in five other nonaqueous solvents. (See later sections of this paper.)

Thin-layer spectroelectrochemical experiments were carried out during controlled-potential oxidation and reduction of $((CN)_4TPP)Co$ in pyridine. The Soret band of $((CN)_4TPP)Co^{II}$ in neat pyridine is split into two peaks, which occur at 438 and 448 nm. The spectrum is similar to that in CH_2Cl_2/py mixtures (see Table I).

A well-defined new spectral band formed at 472 nm as the potential was scanned through peak 1c (−0.05 to +0.25 V). There was also a broad Q-band, which appeared at 672 nm and seemed to consist of two overlapping peaks, which are at about 650 and 680 nm. However, there were well-defined isosbestic points in the oxidation, thus ruling out the possibility of two oxidation products. Also, reversal of the potential scan resulted in a complete regeneration of the original Co(II) spectrum.

Figure 5 shows spectra obtained during the stepwise reduction of $((CN)_4TPP)Co$ in py. Both the first reduction and the second reduction were characterized as reversible one-electron-transfer processes, which occur at half-wave potentials of −0.51 and −0.94 V vs. SCE. Interestingly, the intensity of the Soret and Q-bands of the Co(II) species decreased during the first reduction (Figure 5a). The Q-band absorption reformed after the second reduction process, but the characteristic Soret band of a metalloporphyrin was no longer present. This is shown in Figure 5b.

Figure 5c shows the spectral changes that occurred during the third one-electron reduction. The half-wave potential in pyridine (−1.75 V vs. SCE) is at the edge of the solvent potential limit, and there were large background currents from the py/TBAP system. However, time-resolved spectral changes showed good isosbestic behavior. A new absorption peak appeared at 683 nm during this third reduction, and the original absorption peaks at 443, 585 and 629 nm decreased in intensity. However, if the electrode potential was held at −1.96 V for a long time period, the new absorption peak at 683 nm also decreased in intensity, suggesting either decomposition of the complex or reaction of the

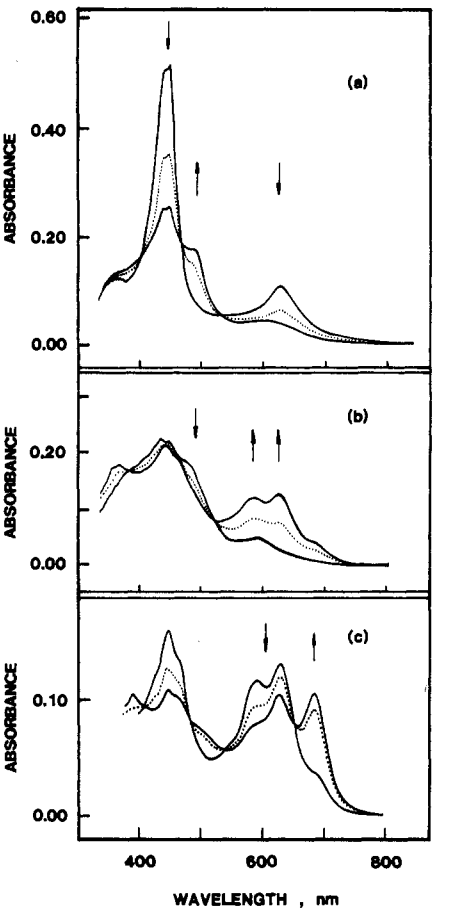

Figure 5. Thin-layer spectral changes associated with reduction of $((CN)_4TPP)Co$ in py containing 0.1 M TBAP. Spectra were monitored as the potential was (a) scanned from −0.13 to −0.56 V (through peak 2a), (b) scanned from −0.71 to −1.18 V (through peak 3), and (c) stepped from −1.18 to −1.96 V (through peak 4).

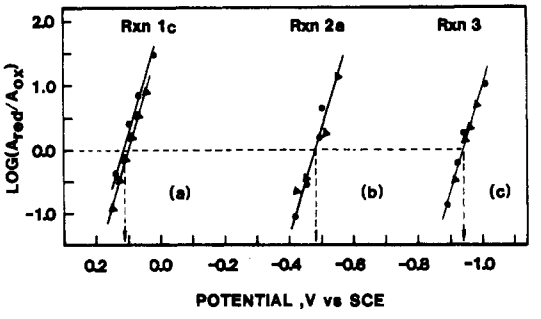

Figure 6. Logarithmic analysis of the spectral data in Figure 6. Reactions 1c, 2a, and 3 were monitored at 472, 446, and 629 nm, respectively, and are identified in Figure 4. Identical spectra were obtained on the negative sweep (▲) and on the positive sweep (●).

trianionic species with the solvent.

Diagnostic plots of the absorbance changes vs. potentials are shown in Figure 6 for each of the three electrode reactions and give slopes of 60 ± 5 mV. Reaction 1c was monitored at 472 nm while eactions 2a and 3 were monitored at 446 and 629 nm, respectively. This type of plot demonstrates the spectral reversibility of the reactions under the given experimental conditions. Also, from the zero intercept of the plots, the half-wave potentials were determined as 0.12, −0.48, and −0.94 V, respectively. These values are close to those obtained by conventional cyclic voltammetry at a Pt electrode. In addition, identical spectra were obtained on the negative potential sweep (▲) and on the reverse positive potential sweep (●), giving further evidence for the reversibility of the reactions.

Spectral changes were also monitored during the two reductions of $((CN)_4TPP)Co^{II}$ in CH_2Cl_2 containing 0.1 M TBAP. The

Table III. Half-Wave Potentials for Reduction of $((CN)_4TPP)Co$

solvent	ACN[a]	DN[a]	ϵ[b]	$E_{1/2}$, V vs. SCE	vs. Fc^+/Fc	vs. SCE	vs. Fc^+/Fc	vs. SCE	vs. Fc^+/Fc
THF	8	20	7.4	−0.30	−0.80	−0.90	−1.40	−1.77	−2.27
HMP	10.6	38.8	29.6	−0.25	−0.80	−0.84	−1.39	−1.78	−2.33
DMA	13.6	27.8	37.8	−0.21	−0.71	−0.82	−1.32	−1.72	−2.22
py	14.2	33.1	12.3	−0.51	−0.99	−0.94	−1.42	−1.75	−2.23
DMF	16	26.6	36.7	−0.24	−0.74	−0.82	−1.32	−1.75	−2.25
PC	18.3	15.1	69	−0.25	−0.61	−0.86	−1.22		
Me_2SO	19.3	29.8	46.7	−0.33	−0.80	−0.80	−1.27	−1.73	−2.20
CH_2Cl_2	20.4		9	−0.21	−0.69	−0.94	−1.42		
NMF	32.1	27	182.4	−0.39	−0.78	−0.84	−1.23		

[a] Taken from: Gutmann, V.; Wychera, E. *Inorg. Nucl. Chem. Lett.* **1966**, *2*, 257. Gutmann, V. *The Donor Acceptor Approach to Molecular Interactions*; Plenum: New York, 1978. [b] Taken from: Born, M. *Z. Phys.* **1920**, *45*, 1.

neutral $((CN)_4TPP)Co$ complex has a Soret band at 434 nm and a Q-band at 626 nm. The first reduction at −0.21 V results in a significant reduction of the Soret band intensity (see Table I) while the Q-band at 589 nm remains intense. After the addition of two electrons to the complex, the Soret band is much reduced in intensity. This is similar to the case for reduction of $((CN)_4TPP)Co$ in pyridine (see Figure 5b and Table I). In addition, there is a new absorption peak at 663 nm while the original absorption peak at 589 nm remains intense.

The above data suggest that the first reduction of $((CN)_4TPP)Co^{II}$ in both pyridine and CH_2Cl_2 is at the porphyrin π ring system rather than at the metal center. Potential differences between the first and the second ring reduction of different metalloporphyrins have been found to average 0.42 ± 0.04 V.[9,32] However, in the case of $((CN)_4TPP)Co^{II}$, a separation of 0.73 mV is measured between the two reductions. This suggests that the second reduction of $((CN)_4TPP)Co$ corresponds to formation of a Co(I) π anion radical in both CH_2Cl_2 and py. Generally, the metal-centered reductions of metalloporphyrins occur at potentials more positive than those for formation of the anion radical and dianion.[1] However, this is not always the case. For example, $((CN)_4TPP)Cu^{II}$ is reduced first to an anion radical and then to a dianion before the generation of Cu(I).[25]

Solvent Effects on $((CN)_4TPP)Co^{II}$ Electrode Reactions. The electroreduction and oxidation of $((CN)_4TPP)Co$ was investigated in eight different nonaqueous solvents. The oxidations were poorly defined in all solvents except pyridine and Me_2SO (see Figure 3d for voltammogram in py). In all other solvents the anodic oxidation peak was not directly coupled to the rereduction peak. This is due to a rate-determining change in coordination number that accompanies the transformation of $((CN)_4TPP)Co^{II}$ to $[((CN)_4TPP)Co^{III}]^+$.

In contrast, the reductions of $((CN)_4TPP)Co$ were very well-defined in all of the investigated solvents, and either two or three reduction processes were observed. Examples of voltammograms in three solvents are given in Figure 7, and a summary of half-wave potentials for the electroreductions of $((CN)_4TPP)Co$ are listed in Table III. Key solvent parameters such as solvent donor number (DN), acceptor number (ACN) and dielectric constants (ϵ) are also listed in this table. The values of $E_{1/2}$ are reported vs. SCE as well as vs. an internal reference standard, which in this case is the ferrocene/ferrocenium couple (Fc/Fc^+).

Three reductions of $((CN)_4TPP)Co$ are observed in THF and HMP and these occur at virtually identical potentials vs. SCE. A third reduction of $((CN)_4TPP)Co$ also occurs in DMA, py, DMF, PC, and Me_2SO but not in CH_2Cl_2 or NMF where potentials for formation of the trianionic species are shifted beyond the potential range of these later solvents.

The effect of solvents on half-wave potentials for the oxidation of (TPP)Co has been discussed in the literature.[5,6,12,33] Changing from a nonbonding solvent such as CH_2Cl_2 to solvents of higher coordinating ability leads to substantial negative shifts in $E_{1/2}$ for

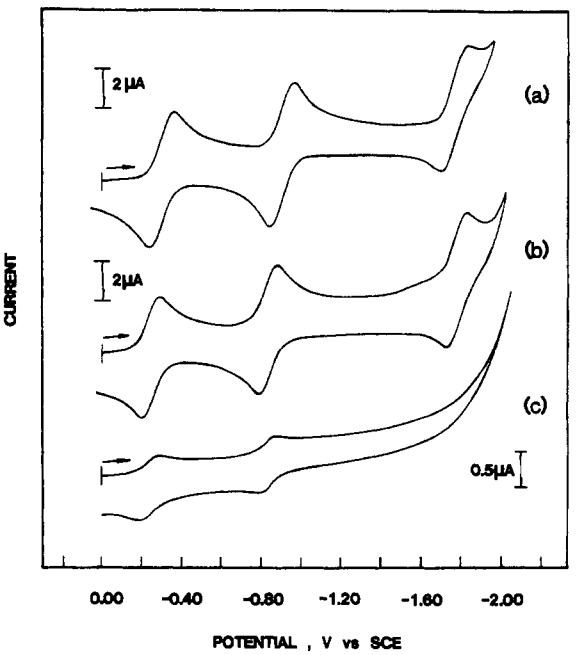

Figure 7. Cyclic voltammograms of $((CN)_4TPP)Co$ at a Pt electrode in (a) THF, (b) HMP, and (c) PC containing 0.1 M TBAP.

the Co(II) ⇄ Co(III) reaction. These shifts of $E_{1/2}$ are due to the larger stabilization of Co(III) than Co(II) upon solvent binding and are over 1.0 V in magnitude. Good correlations have been obtained between $E_{1/2}$ for oxidation of $(TPP)Co^{II}$ and the Gutmann donor number of the solvent,[33] and this is consistent with stabilization of the positively charged Co(III) complex. Good correlation of $E_{1/2}$ with Gutman donor number is also observed for the M(II)/M(III) reactions of $(TPP)M^{II}$, where M = Mn[34] and Fe,[35] but the largest solvent effect (determined by $\Delta E_{1/2}/\Delta(DN)$) is for complexes of cobalt.[33]

There is a very small solvent dependence on half-wave potentials for reduction of $(TPP)Co^{II}$.[1,5,6,12] This is consistent with a decreased interaction between the solvent and the neutral or reduced forms of the complex. $(TPP)Co^{II}$ porphyrins bind most nonaqueous solvents only weakly[12] while $[(TPP)Co^{I}]^-$ has little interaction with solvents which do not axially complex to the cobalt metal ion.

In this present study we have investigated the three reductions of $((CN)_4TPP)Co$ in nine nonaqueous solvents. A detailed report of how different solvents effect metalloporphyrin electrode reactions concludes that the best solvent parameter for evaluating trends in reductions of metalloporphyrins is the Gutmann acceptor number (ACN) rather than the Gutmann donor number.[36] In this present study we have evaluated shifts of $E_{1/2}$ vs. the ACN,

(32) Fuhrhop, J.-H.; Kadish, K. M.; Davis, D. G. *J. Am. Chem. Soc.* **1973**, *95*, 5140.
(33) Kadish, K. M.; Bottomley, L. A.; Kelly, S.; Schaeper, D.; Shiue, L. R. *Bioelectrochem. Bioenerg.* **1981**, *8*, 213.
(34) Kelly, S.; Kadish, K. M. *Inorg. Chem.* **1982**, *21*, 3631.
(35) Bottomley, L. A.; Kadish, K. M. *Inorg. Chem.* **1981**, *20*, 1348.
(36) Kadish, K. M.; Cornillon, J.-L.; Yao, C.-L.; Malinski, T.; Gritzner, G., manuscript in preparation.

the DN, and the solvent dielectric constant (ϵ), but in all three cases no good correlations were obtained. Solvents of higher donor number (HMP and py) as well as high acceptor number (NMF) were utilized, but no well-defined correlations were observed. This is similar to the case of $((CN)_4TPP)FeCl$[26] and is most likely due to the poor binding ability of the different solvents to reduced $((CN)_4TPP)Co$.

Acknowledgment. Support of the National Science Foundation (Grant No. CHE-8515411) is gratefully acknowledged. We also acknowledge helpful discussions with Dr. Madhav Chavan.

Registry No. $((CN)_4TPP)Co^{II}$, 71147-59-6; $((CN)_4TPP)Co^{II}(py)$, 103190-70-1; $((CN)_4TPP)Co^{II}(py)_2$, 103190-71-2; $[((CN)_4TPP)Co^{III}]^+$, 103190-72-3; $[((CN)_4TPP)Co^{III}(py)_2]^+$, 103200-96-0; $[((CN)_4TPP)Co^{II}]^-$, 103190-73-4; $[((CN)_4TPP)Co^{II}(py)]^-$, 103190-74-5; $[((CN)_4TPP)Co^{I}]^{2-}$, 103190-75-6; $[((CN)_4TPP)Co^{I}]^{3-}$, 103190-76-7; pyridine, 110-86-1.

Contribution from the Department of Chemistry, Purdue University, West Lafayette, Indiana 47907

Three Forms of a Copper(III) Tripeptideamide and a Comparison of Their Photochemistry

Joanna P. Hinton and Dale W. Margerum*

Received April 9, 1986

Tri-α-aminoisobutyryl amide, Aib_3a, forms three square-planar copper(III) complexes that are stable (25 °C, in the dark) in aqueous solution from pH 0 to 14, where H_{-n} refers to the number of coordinated deprotonated nitrogens:

$$Cu^{III}(H_{-2}Aib_3a)^+ \xrightleftharpoons{pK_a = 0.25} Cu^{III}(H_{-3}Aib_3a) \xrightleftharpoons{pK_a = 12.5} Cu^{III}(H_{-4}Aib_3a)^-$$

The predominant form (pH 0.25-12.5) has an amine nitrogen, two deprotonated peptide nitrogens, and a deprotonated amide nitrogen coordinated to copper(III). In strong acid the terminal amide nitrogen is protonated, and coordination to the metal is by the amide oxygen. In strong base the amine nitrogen is deprotonated and remains coordinated to copper(III). In contrast to their stability with respect to redox decomposition, these complexes show varied photochemical sensitivity upon irradiation into their ligand-to-metal charge-transfer (LMCT) bands. Coordination by an amine nitrogen and three deprotonated amide nitrogens enhances photochemical loss of copper(III) in the UV-LMCT band ($\Phi = 0.34$) relative to coordination by an amine nitrogen, two deprotonated amide nitrogens, and a carbonyl oxygen ($\Phi = 0.30$). The opposite dependence is observed upon irradiation in the visible-LMCT band, where $\Phi = 0.16$ for $Cu^{III}(H_{-3}Aib_3a)$ and $\Phi = 0.22$ for $Cu^{III}(H_{-2}Aib_3a)^+$. Deprotonation of the terminal amine nitrogen causes a dramatic reduction in the quantum yield with $\Phi \leq 0.004$ in the visible region and 0.08 in the UV region. The photodecomposition products vary for the three complexes and are wavelength-dependent. The principal peptide oxidation products from photolysis of $Cu^{III}(H_{-3}Aib_3a)$ at pH 5 and $Cu^{III}(H_{-4}Aib_3a)^-$ in 1.0 M OH^- are substituted hydantoins, which are proposed to form by a metal-assisted intramolecular nucleophilic reaction. The different photodecomposition mechanisms are discussed.

Introduction

Stabilization of trivalent copper is no longer considered unusual. A variety of donor groups have been used to coordinate copper in this high oxidation state, including deprotonated peptide nitrogens,[1-4] amidate nitrogens,[5] sulfur groups,[6-9] and macrocyclic polyamine, amide, imide, and azine nitrogens.[10-15] These copper(III) complexes have been characterized by X-ray crystallography,[4,5,7,9,11] EXAFS,[16] electrochemistry,[2,5,8,14,17] proton- and electron-transfer reactions,[18-28] and their photochemical behavior.[3,8,29]

Bis(dithiooxalato-*S*,*S*')copper(III) is reported to undergo a light-activated, intramolecular ligand-to-copper two-electron transfer with cleavage of the C-C bond in the ligand and generation of gaseous SCO.[8] Copper(III) peptides also undergo photoinduced redox decomposition upon irradiation of their lig-

(1) Margerum, D. W.; Chellappa, K. L.; Bossu, F. P.; Burce, G. L. *J. Am. Chem. Soc.* **1975**, *97*, 6894-6896.
(2) Bossu, F. P.; Chellappa, K. L.; Margerum, D. W. *J. Am. Chem. Soc.* **1977**, *99*, 2195-2203.
(3) Kirskey, S. T., Jr.; Neubecker, T. A.; Margerum, D. W. *J. Am. Chem. Soc.* **1979**, *101*, 1631-1633.
(4) Diaddario, L. L.; Robinson, W. R.; Margerum, D. W. *Inorg. Chem.* **1983**, *22*, 1021-1025.
(5) Birker, P. J. M. W. L. *Inorg. Chem.* **1977**, *16*, 2478-2482.
(6) Wijinhoven, J. G.; van den Hark, T. E. M.; Beurskers, P. T. *J. Cryst. Mol. Struct.* **1972**, *2*, 189-196.
(7) Coucouvanis, D.; Hollander, F. J.; Caffery, M. L. *Inorg. Chem.* **1976**, *15*, 1853-1860.
(8) Imamura, M. R.; Gordon, G.; Coucouvanis, D. *J. Am. Chem. Soc.* **1984**, *106*, 984-990.
(9) Kanatzidis, M. G.; Baenziger, N. C.; Coucouvanis, D. *Inorg. Chem.* **1985**, *24*, 2680-2683.
(10) Rybka, J. S.; Margerum, D. W. *Inorg. Chem.* **1981**, *20*, 1453-1458.
(11) Oliver, K. J.; Waters, T. N. *J. Chem. Soc., Chem. Commun.* **1982**, 1111-1112.
(12) Olson, D. C.; Vasilevski, J. *Inorg. Chem.* **1971**, *10*, 463-470.
(13) Sulfab, Y.; Al-shatti, N. A. *Inorg. Chem.* **1984**, *87*, L23-L24.
(14) Castellani, C. B.; Fabbrizzi, L.; Licchelli, M.; Perotti, A.; Poggi, A. *J. Chem. Soc., Chem. Commun.* **1984**, 806-808.
(15) Kimura, E.; Sakonaka, A.; Nakamoto, M. *Biochim. Biophys. Acta* **1981**, *678*, 172-179.
(16) Kennedy, W. R.; Powell, D. R.; Niederhoffer, E. C.; Teo, B.-K.; Orme-Johnson, W. H.; Margerum, D. W., to be submitted for publication.
(17) Youngblood, M. P.; Margerum, D. W. *Inorg. Chem.* **1980**, *19*, 3068-3072.
(18) Rybka, J. S.; Kurtz, J. L.; Neubecker, T. A.; Margerum, D. W. *Inorg. Chem.* **1980**, *19*, 2791-2796.
(19) Neubecker, T. A.; Kirksey, S. T., Jr.; Chellappa, K. L.; Margerum, D. W. *Inorg. Chem.* **1979**, *18*, 444-448.
(20) Owens, G. D.; Chellappa, K. L.; Margerum, D. W. *Inorg. Chem.* **1979**, *18*, 960-966.
(21) DeKorte, J. M.; Owens, G. D.; Margerum, D. W. *Inorg. Chem.* **1979**, *18*, 1538-1542.
(22) Lappin, A. G.; Youngblood, M. P.; Margerum, D. W. *Inorg. Chem.* **1980**, *19*, 407-413.
(23) Koval, C. A.; Margerum, D. W. *Inorg. Chem.* **1981**, *20*, 2311-2318.
(24) Anast, J. M.; Margerum, D. W. *Inorg. Chem.* **1982**, *21*, 3494-3501.
(25) Anast, J. M.; Hamburg, A. W.; Margerum, D. W. *Inorg. Chem.* **1983**, *22*, 2139-2145.
(26) Owens, G. D.; Phillips, D. A.; Czarnecki, J. J.; Raycheba, J. M. T.; Margerum, D. W. *Inorg. Chem.* **1984**, *23*, 1345-1353.
(27) Dennis, C. R.; Nemeth, M. T.; Kumar, K.; Margerum, D. W., to be submitted for publication.
(28) Kumar, K.; Rotzinger, F. P.; Endicott, J. F. *J. Am. Chem. Soc.* **1983**, *105*, 7064-7074.
(29) Hamburg, A. W.; Margerum, D. W. *Inorg. Chem.* **1983**, *22*, 3884-3893.

0020-1669/86/1325-3248$01.50/0 © 1986 American Chemical Society